

A Framework for Routing DNN Inference Jobs over Distributed Computing Networks

Sehun Jung
Dept. of CSE, Konkuk University
Seoul, Republic of Korea
qhs11213@konkuk.ac.kr

Hyang-Won Lee
Dept. of CSE, Konkuk University
Seoul, Republic of Korea
leehw@konkuk.ac.kr

Abstract—Ubiquitous artificial intelligence (AI) is considered one of the key services in 6G systems. AI services typically rely on deep neural network (DNN) requiring heavy computation. Hence, in order to support ubiquitous AI, it is crucial to provide a solution for offloading or distributing computational burden due to DNN, especially at end devices with limited resources. We develop a framework for assigning the computation tasks of DNN inference jobs to the nodes with computing resources in the network, so as to reduce the inference latency in the presence of limited computing power at end devices. To this end, we propose a layered graph model that enables to solve the problem of assigning computation tasks of a single DNN inference job via simple conventional routing. Using this model, we develop algorithms for routing DNN inference jobs over the distributed computing network. We show through numerical evaluations that our algorithms can select nodes and paths adaptively to the computational attributes of given DNN inference jobs in order to reduce the end-to-end latency.

I. INTRODUCTION

6G system is envisioned to support artificial intelligence (AI) services all over the network from the core to the end hosts, referred to as ubiquitous AI [1]. In many cases, AI services depend on the computation of deep neural network (DNN) and hence require a fair amount of computing power, even only for inference. This can be a significant burden especially for end devices such as mobile phones and IoT devices in which computing resources are highly limited as they run on limited battery power. In order for ubiquitous AI service to be in place, it is thus necessary to provide a solution to overcome limited computing power.

There are several approaches to enable AI at end devices. One is to find a lightweight NN architecture commensurate with available computing resources. SqueezeNet in [2] makes extensive use of 1x1 convolutions to reduce the number of parameters. MobileNetV1 in [3] reduces the number of arithmetic operations by introducing depth-wise separable convolutions. In [4], automated neural architecture search (NAS) is proposed based on reinforcement learning in which the reward reflects the latency of inference. Since the latency depends on the underlying computing resources, such a reward drives the action (i.e., values of hyperparameters) toward the set of architectures that can yield reasonably fast inference for

given computing power. There is a large body of work in this context, and refer to [5] for more details.

Another approach is to exploit computing resources dispersed over the network. Specifically, the (feedforward) computation of DNN inference job is partitioned into multiple tasks, and these computation tasks are assigned to nodes with computing resources in the physical network. For example, in layer-wise partition, all the neurons in the same layer are assigned to a same node. Once a node finishes computing the task(s) assigned, it transfers the output data (of the corresponding DNN layer) to the next node and subsequently, the transferred data are fed as the input data to the corresponding layer. In this work, we consider the problem of assigning computation tasks to nodes and routing data between layers.

Many of works in this context consider the Inter-of-Things (IoT) environment in which nodes are equipped with limited computing resources. In [6], each hidden neuron is mapped to an IoT node. The goal is to find a mapping that minimizes the network-wide total transmit power or time while the computing resource needed for assigned neurons and daily energy consumption satisfy the specified limit. The work of [7] assumes layer-wise partition, and seeks to find a mapping that minimizes (data) transmission time plus computation time, subject to privacy constraints as well as various resources constraints. This problem is formulated as an integer quadratic program, and a reinforcement learning based mapping algorithm is proposed. In [8], a similar problem and formulation are developed with early-exit convolutional neural network (CNN). Some work considers vertical partition of convolution operations that take the majority of computation in DNN. Unlike the layer-wise partition where partitioned tasks have precedence constraint, in vertical partition, convolution operations are partitioned into tasks that can be computed independently. In [9], an IoT node distributes such independent computation tasks (formed through vertical partition) to nearby IoT devices and fuses the collected results at the output of convolution layer. There are also some work considering both vertical and layer-wise partitions together with model sparsification [10].

In this work, we develop a framework for routing DNN inference jobs with a focus on end-to-end latency, defined as the duration between the time when the data at source start to be processed and the time when the inference result

This work was supported by the National Research Foundation of Korea (NRF) grant funded by the Korea government (MSIT) (No.2021R1A2C2012801). (Corresponding author: Hyang-Won Lee)

is delivered to the destination. Obviously, the end-to-end inference latency consists of waiting time and service time. The waiting occurs at link(s) when data need to wait to be transmitted, and also at node(s) when computation tasks need to wait to be processed. The service time is the pure transmission time plus computation time. With this definition, most of the existing works mentioned above focus primarily on minimizing the service time while it is also important to take into account the waiting time.

It is generally hard to deal with waiting time as it is a complex function of arrivals and departures. Nonetheless, we consider a fictitious system in which the waiting time is an upper bound on the waiting time in the actual system. We also propose a layered graph (of the original computing network) in which the conventional routing (without computing components) gives a path over the original computing network that specifies the node for the computation of each DNN layer as well as a path from source to destination. This layered graph together with the fictitious system greatly simplifies the routing of a single DNN inference job. We develop some algorithms in this framework and demonstrate the performance.

The rest of the paper is organized as follows. In Section II, we present the system model and describe the problem. In Section III, the layered graph model is proposed together with the integer linear program (ILP) formulation for routing a single DNN inference job. We prove that the ILP is easy to solve. In Section IV, we develop algorithms for routing multiple DNN inference jobs by exploiting the layered graph and ILP formulation. In Section V, we present numerical results that validate our framework. We conclude the paper in Section VI.

II. SYSTEM MODEL AND PROBLEM DESCRIPTION

Consider a communication network in which some nodes are equipped with computing resources. Let $G_p = (V_p, E_p)$ denote this physical network where V_p is the set of nodes (routers/servers/hosts) and E_p is the set of edges (communication links) connecting the nodes. Let μ_{uv} be the transmission capacity of link $(u, v) \in E_p$. The computation capacity of node u is denoted as μ_u , and its unit is assumed to be GFLOPs/sec. There is a queue for every transmission link, and Q_{uv} is the queue length at link (u, v) representing the amount of packets waiting to be transmitted. Likewise, Q_u is the amount of computation tasks (in GFLOPs) waiting to be computed at node u . This computing network is used to process deep neural network (DNN) inference jobs.

A. Inference Jobs

There are J DNN inference jobs, each corresponding to the feedforward computation of a DNN model¹. For each model j , the input data (e.g., camera images and sensor values) are generated at $s^j \in V_p$ and the inference result needs to be delivered to $t^j \in V_p$. Each model $j (= 1, \dots, J)$ has L_j layers. We assume that each layer can be possibly computed

at different nodes in V_p . Let c_{jl} be the load of computing layer $l (= 1, \dots, L_j)$ of model j . Hence, $\frac{c_{jl}}{\mu_u}$ is the *computation time* if layer l of model j is to be processed at node u . Let d_{jl} be the output data size of layer l of model j . Similarly, $\frac{d_{jl}}{\mu_{uv}}$ is the *transmission time* if the output data of layer l is to be transferred from node u to v . The computation time plus transmission time is called the *service time*. Hence, if layer l of model j is computed at node u , and the output data is transferred to node v , then the service time at this segment is $\frac{c_{jl}}{\mu_u} + \frac{d_{jl}}{\mu_{uv}}$.

We also consider the *waiting time*. In the above example, suppose that the queue length at node u is Q_u when the computation task arrives at node u , and the queue length at link (u, v) is Q_{uv} when the output of computation is buffered at link (u, v) for transmission. Thus, the waiting time is $\frac{Q_u}{\mu_u} + \frac{Q_{uv}}{\mu_{uv}}$. The duration between the time of entering node u and the time of arriving at node v is waiting time plus service time, i.e., $\frac{Q_u}{\mu_u} + \frac{Q_{uv}}{\mu_{uv}} + \frac{c_{jl}}{\mu_u} + \frac{d_{jl}}{\mu_{uv}}$. In this work, for simplicity of presentation, we ignore propagation time at any component either inside a node or between nodes (i.e., link), but our results can be readily applied to the scenario with propagation delay as propagation adds constant delay.

B. Job Completion Time

Suppose that each job j is assigned a path from its source s^j to destination t^j , including the information of the node at which each layer is computed. Time starts from 0. Let C_j be the time when the inference result of job j is delivered to the destination, i.e., t^j . Hence, C_j is the end-to-end inference latency. This time is obviously equal to waiting time plus service time along the path from s^j to t^j . Define the *job completion time* C_{\max} as

$$C_{\max} = \max_j C_j.$$

Hence, C_{\max} is the time when all the jobs are finished. This time is also called *makespan* in the field of job-shop scheduling. Clearly, the job completion time is determined by path selection for data transfer and node selection for computation. We simply call these two decisions “routing”.

In this work, we develop algorithms for routing interference jobs for minimum job completion time. Fig. 1 shows an example of routing policies. There are two inference jobs, one from s^1 to t^1 requiring 25GFLOPs and another from s^2 to t^2 requiring 50GFLOPs. For simplicity of discussion, assume that there is only one layer in the corresponding DNN model, and that there is no transmission delay. The computing resources are only at node u with 25GFLOPs/s and node v with 50GFLOPs/s. Routing policy 1 seeks to minimize the service time. As a consequence, both of two inference jobs are processed at node v . The total service time is 1.5s, and the job completion is 1.5s as well since either job 1 or 2 must wait at node v until the other is finished. On the other hand, routing policy 2 seeks to minimize the job completion time by taking into account waiting time. Since processing both jobs at node v incurs waiting, it assigns disjoint paths.

¹We call job and model interchangeably depending on the context

Although the total service time is 2s, the job completion time is reduced to 1s, compared to 1.5s under routing policy 1. This example shows that minimizing the total service time can potentially result in an extreme solution where jobs are processed only at a small number of nodes (which incurs extra delay in job completion). Clearly, in order to reduce the job completion time, one needs to somehow account for the waiting time. As mentioned in Section I, most of the previous work in the context of distributed DNN computation focuses on minimizing service time.

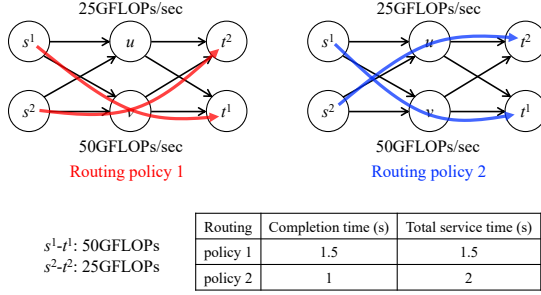


Fig. 1. Example of routing policies (ignoring transmission time)

C. Challenges

There are several challenges in tackling the problem of routing DNN inference jobs for minimum completion time. First, the routing problem in this work is inherently related to the classical job-shop scheduling problem which is known to be NP-complete [11]. In the job-shop scheduling problem, there are multiple jobs, and each job consists of ordered operations. All of the operations must be assigned to some process, and in each process, the priority among operations should be decided in order to minimize the job completion time. If the process for each operation to be computed is given and fixed, then the problem is called the “job-shop scheduling problem”. Otherwise, it is called the “flexible job-shop scheduling problem”. In our problem, each layer (corresponding to operation in job-shop scheduling) in every job should be assigned a node for computation, together with path selection. Our problem therefore contains a flexible job-shop scheduling which is hard to solve. Note that this is immensely different from the conventional routing problem which is easy to solve under many circumstances. We develop heuristic algorithms based on the layered graph representation of the problem.

Another challenge comes from the difficulty of handling waiting time. It is necessary to predict the waiting time so that the routing decision can be made by taking into account both waiting time and service time. However, the waiting time at a component (i.e., node or link) depends on the departure processes in the preceding components and hence, it is hard to predict the waiting time. To circumvent this issue, we consider a fictitious system in which the waiting time provides an upper bound on the actual waiting time. The completion time in the fictitious system is thus an upper bound on the actual completion time. We seek to minimize the upper bound on the completion time. The details are presented in Section III.

III. LAYERED GRAPH AND FORMULATION

As mentioned above, our problem requires to determine the path as well as the node for computation. It is hard to formulate this problem applying the traditional technique involving flow conservation constraints. Inspired by [12] and [13], we construct the layered graph with which the problem can be simplified. In this section, we address the problem of routing a single model with L layers (the case of multiple models is fully addressed in Section IV). Consider $L + 1$ copies of G_p , named G_0, G_1, \dots, G_L with $G_l = (V_l, E_l), \forall l$. For each $l = 0, \dots, L$, denote by $u_l \in G_l$ the replicated node of $u \in G_p$, and hence, $(u_l, v_l) \in G_l$ the replicated link of $(u, v) \in G_p$. There is an edge from node u_{l-1} to u_l for all $u \in G_p$ and $l = 1, \dots, L$. These edges are called *cross-layer edges*, denoted by E_c . Define the layered graph $G = (V, E)$ where $V = V_0 \cup \dots \cup V_L$ and $E = E_0 \cup \dots \cup E_L \cup E_c$. Fig. 2 shows an example of the layered graph G derived from the original physical network graph G_p .

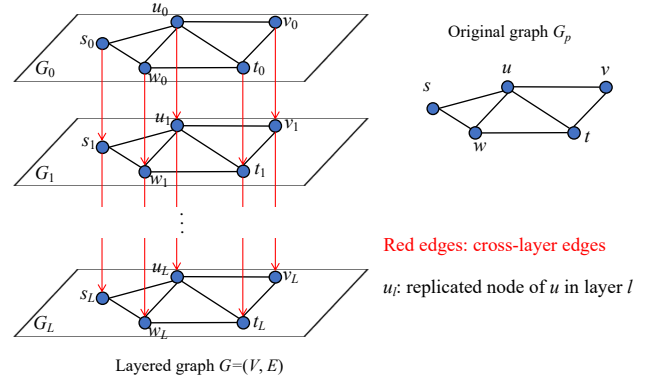


Fig. 2. Example of layered graph for L layers in the DNN model

A. Routing in Layered Graph

We now discuss how the routing in the layered graph simply expresses both path selection for data transfer and node selection for computation. Suppose that source and destination nodes are $s \in V_p$ and $t \in V_p$ respectively. Consider finding a path from s_0 to t_L . The cross-layering segment of the path specifies the node where the corresponding layer is computed. For instance, if the path traverses link (u_{l-1}, u_l) , then layer l of the model is computed at node u . The intra-layer segment of the path specifies the transfer of the output data of corresponding layer (of model). For instance, if the path traverses the link (u_l, v_l) , then the output data of layer l is transferred from node u to node v . Fig. 3 shows an example of routing in the layered graph, and what each segment in the path represents. It is important to note that the classical routing (that just finds a path from source to destination) in the layered graph determines both path selection and node selection for computing of all the layers of the model simultaneously.

B. Formulation with Upper Bounds on Waiting Time

We assume preemptive scheduling at links and nodes. Priority is assigned to every inference “job” (not to individual layers), and uniformly applied to all the layers belonging

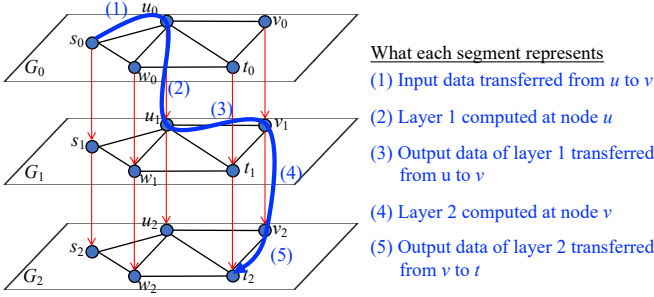


Fig. 3. Example of routing in layered graph with $L = 2$

to the same job. For instance, consider two jobs j_1 and j_2 , and suppose that job j_1 has higher priority than job j_2 . The computation/transmission task of a layer in job j_2 can be preempted (while it is being computed or transmitted) up on the arrival of the computation/transmission task of job j_1 .

Recall that we need to determine the routing of a single model. Suppose that the queue lengths $Q_u, \forall u \in V_p$ and $Q_{uv}, \forall (u, v) \in E_p$ are the computation and transmission tasks (that are already routed) with higher priority than the current model to be routed. These queue lengths as well as capacities in the physical network are reflected into the layered graph as follows:

- 1) $Q_{u_l v_l} = Q_{uv}, \forall (u, v) \in E_p, l = 0, 1, \dots, L$
- 2) $Q_{u_{l-1} u_l} = Q_u, \forall u \in V_p, l = 1, \dots, L$
- 3) $\mu_{u_l v_l} = \mu_{uv}, \forall (u, v) \in E_p, l = 0, 1, \dots, L$
- 4) $\mu_{u_{l-1} u_l} = \mu_u, \forall u \in V_p, l = 1, \dots, L$
- 5) $q_{uv} = \begin{cases} d_l, & \text{if } (u, v) \in E_l, l = 0, \dots, L \\ c_l, & \text{if } (u, v) = (w_{l-1}, w_l) \in E_c, l = 1, \dots, L \end{cases}$

Namely, the replicated edges have the same queue length and capacity as in the original network, and the cross-layer edges reflect the node queue length and capacity (so that traversing a cross-layer edge is equivalent to computing at the corresponding node).

Define the variable r_{uv} to be 1 if the path traverses edge $(u, v) \in E$, and 0 otherwise. The routing problem can be formulated as follows:

$$\min_{r, z} \sum_{(u, v) \in E} \frac{q_{uv}}{\mu_{uv}} r_{uv} + \sum_{u \in V_p} \frac{Q_u}{\mu_u} z_u + \sum_{l=0}^L \sum_{(u, v) \in E_l} \frac{Q_{uv}}{\mu_{uv}} r_{uv} \quad (1)$$

$$\text{s.t. } z_u \geq r_{u_{l-1} u_l}, \forall u \in V_p, l = 1, \dots, L \quad (2)$$

$$\sum_{v: (u, v) \in E} r_{uv} - \sum_{v: (v, u) \in E} r_{vu} = \begin{cases} 1, & \text{if } u = s_0 \\ -1, & \text{if } u = t_L, \forall u \in V \\ 0, & \text{otherwise} \end{cases} \quad (3)$$

$$r_{uv} \in \{0, 1\}, \forall (u, v) \in E \quad (4)$$

$$z_u \in \{0, 1\}, \forall u \in V \quad (5)$$

Constraint (3) requires that a path from s_0 to t_L should be found. As discussed above, this is equivalent to finding a path from s to t in the physical network, together with node selection for computing L layers of the model.

The first term in (1) represents the total service time at nodes and links. By constraint (2), z_u is 1 in the optimal solution

only if node u is selected for computing layer(s). The second term is thus the total waiting time at nodes, assuming that the computation of the current job at each node u must wait until all the computation tasks of higher priority. This is obviously an upper bound on the actual waiting time because some of the computation tasks in Q_u may have been finished by the time when the computation task of the current job arrives at the node. Similarly, the third term in (1) is an upper bound on the total waiting time at links. The objective function in (1) is thus an upper bound on the actual service time plus waiting time which is equal to the completion time. Therefore, the above formulation seeks to find a routing that minimizes an upper bound on the job completion time.

Due to networking delays (i.e., transmission times), it is hard to express the actual waiting time in a simple form. The upper-bound approach enables a simple formulation. Although there may be a gap between upper bound and actual completion time, we expect that minimizing the upper bound would have the effect of minimizing the actual job completion time. In the following, we consider this fictitious system in which the upper bound is treated as the actual waiting time.

ILP is NP-hard to solve in general. However, we show that our formulation has a special structure called total unimodularity, so that the optimal solution to ILP can still be found with the relaxation of binarity constraints in (4) and (5), i.e., $0 \leq r_{uv} \leq 1$ and $0 \leq z_u \leq 1$. With this relaxation, the formulation is just a linear program (LP) which is polynomial time solvable.

Theorem 1: The LP relaxation of formulation (1)-(5) has an integral optimal solution (i.e., an optimal single path with minimum completion time).

Proof: See Appendix A. ■

IV. ROUTING ALGORITHMS

In this section, we develop algorithms for routing multiple jobs. We exploit the fact that the single-job problem is easy as shown in the previous section.

A. Greedy Algorithm

Let $Q = [Q_{uv}, \forall (u, v) \in E]$ which is the vector of unfinished transmission/computation tasks in the network. Recall that this vector determines the waiting time of jobs. Let $C_j(Q)$ be the optimal objective function value of formulation (1)-(5) for job j . That is, $C_j(Q)$ is the completion time of job j if it is routed based on the formulation in the presence of unfinished tasks Q . Let $r^*(j)$ be the optimal routing variable in this case.

Algorithm 1 shows the greedy algorithm. First, it computes the completion time of every job, and selects the job with earliest completion time (line 1). This selected job is given highest priority. Second, the unfinished task vector Q is updated (line 2) so that the remaining jobs with lower priority can be routed with updated waiting time. The same procedure is repeated until all the jobs are routed.

The approximation ratio of this algorithm can be derived. Let us abuse the notation by defining $|V_p|$ and $|E_p|$ as the numbers of nodes with positive computation capacity and

Algorithm 1: Greedy Algorithm

Given: J jobs**Init:** $Q_{uv} = 0, \forall (u, v) \in E; U = \{1, \dots, J\}; p = 1;$ **1 while** $U \neq \emptyset$ **do****2** $j_p = \arg \min_{j \in U} C_j(Q);$ **3** $Q_{uv} \leftarrow Q_{uv} + q_{uv} r_{uv}^*(j_p), \forall (u, v) \in E;$ **4** $p \leftarrow p + 1;$ **5** $U \leftarrow U \setminus \{j^*\};$ **6 end****Output:** Priority: $j_1 > \dots > j_J$ Routing: $r_{uv}^*(j_p), \forall (u, v), p = 1, \dots, J$

edges with finite transmission capacity respectively in the original graph G_p . Let T^* be the minimum possible job completion time in the actual system.

Theorem 2: Assume that the graph G_p is k -edge-connected. Then, the job completion time under the greedy algorithm in Algorithm 1 is at most αT^* , where

$$\alpha = \max \left\{ 2\alpha_{tx}, \frac{2(L+1)(|V_p| + |E_p|)\alpha_{tx}}{k}, \left(1 + \frac{|E_p|}{|V_p|}\right) \alpha_{cp} \right\} \left\{ 2 - \frac{1}{|V_p| + |E_p|} \right\}$$

$$\alpha_{tx} = \frac{h_L \cdot \max_{j,l} d_{j,l} \cdot \max_{(u,v)} \mu_{uv}}{h_S \cdot \min_{j,l} d_{j,l} \cdot \min_{(u,v)} \mu_{uv}}, \quad \alpha_{cp} = \frac{\max_{u \in V_p} \mu_u}{\min_{u \in V_p} \mu_u}$$

$$h_L = \max_j h_L^j, \quad h_S = \min_j h_S^j$$

h_L^j = longest path length in G_p in hop count btw. s^j and t^j

h_S^j = shortest path length in G_p in hop count btw. s^j and t^j .

Proof: See Appendix B. ■

Therefore, the greedy policy is an α -approximation algorithm.

Corollary 1: With zero network delay and identical computation capacity at all nodes, the greedy policy is a $(2 - 1/|V_p|)$ -approximation algorithm.

Proof: See Appendix C. ■

Although the approximation ratio in 2 seems loose, in the special case as in Corollary 1, our algorithm approximates the optimal solution within a factor smaller than 2. Recall that the completion time under the greedy policy is an upper bound on the completion time that will be achieved by greedy in the actual system. Hence, the approximation ratio of greedy immediately leads to the approximation of greedy in the actual system. We thus anticipate our algorithm performs well in many other scenarios.

B. Simulated Annealing

We also present a simulated annealing algorithm. Typically, simulated annealing defines the neighborhood of current solution, and a new solution is generated by sampling one of the neighbors uniformly at random. If the new solution improves the objective function value, the new solution is accepted as a current solution. Otherwise, the new solution is accepted

with small probability so as to avoid getting trapped at local optimum. It is important to define the neighborhood in a way that all the solutions can be potentially visited, and also to appropriately cool down the probability of accepting worse solution.

Algorithm 2 shows our simulated annealing based routing algorithm. Let $r(j)$ denote the routing of job j , and $r = [r(j), j = 1, \dots, J]$. Let $P = [j_1, \dots, j_J]$ be the vector representing priority relationship $j_1 > \dots > j_J$. The temperature controlling the exploration probability is denoted as T , and $d < 1$ is a reduction factor. Our simulate annealing alternately samples a neighbor of current solution by either changing a processing node or shuffling priority. In the case of odd iteration number (lines 3-5), we choose a job j , its layer l and processing node w uniformly at random (line 3). The new routing r_{new} is generated by switching the current processing node (in r_{old}) of layer l of job j to node w (line 4), and then, calculate the completion time with the new solution with routing r_{new} (line 5). On the other hand, in the case of even iteration number (lines 7-8), two random selected jobs in the priority vector P_{old} are swapped (line 7), and the completion time is calculated with the new solution with priority P_{new} (line 8). Finally, the new solution solution is accepted with probability $\min(1, e^{\frac{C_{\text{old}} - C_{\text{new}}}{kT}})$ which indeed always accepts if the new solution is better.

Algorithm 2: Simulated Annealing

Given: J jobs;**Init:** $T = 1$; random routing r_{old} and priority P_{old} ;**1 while** $T > T_{\text{lim}}$ **do****2** **if** iteration number is odd **then****3** Choose a job j , its layer l and processing node $w \in V_p$ all uniformly at random;**4** $r_{\text{new}} = \text{updateRoute}(r_{\text{old}}, j, l, w);$ **5** $C_{\text{new}} = \text{calculateCompletionTime}(r_{\text{new}}, P_{\text{old}});$ **6** **else****7** $P_{\text{new}} = \text{swapTwoJobsInP}(P_{\text{old}});$ **8** $C_{\text{new}} = \text{calculateCompletionTime}(r_{\text{old}}, P_{\text{new}});$ **9** **end****10** $r_{\text{old}} \leftarrow r_{\text{new}}$ and $P_{\text{old}} \leftarrow P_{\text{new}}$ with probability $\min(1, e^{\frac{C_{\text{old}} - C_{\text{new}}}{kT}});$ **11** $T \leftarrow T \cdot d;$ **12 end****Output:** Priority: P_{old} Routing: r_{old}

It is important to note that the above two algorithms are an example of routing under our framework, and many other types of algorithms such as reinforcement learning can be developed, which we leave as future study.

V. NUMERICAL EVALUATION

In this section, we compare the greedy policy in Algorithm 1 and simulated annealing in Algorithm 2. We use two topologies including a small topology with five nodes in Fig. 2, and a

large US backbone network shown in Fig. 4. Communication links are all assumed to be bidirectional.

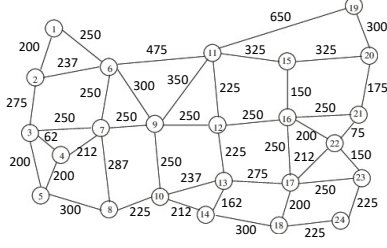


Fig. 4. US backbone network topology. Numbers are capacities in MB/s

For the small topology, there are two DNN models, VGG19 and ResNet34. The amount of computations c_{jl} (FLOPs) in each layer is computed based on the formula in [14]. The memory footprint (i.e., output data size d_{jl}) of each layer can be easily calculated based on the dimension of the output data. We assume that there are eight jobs (i.e., $J = 8$), two VGG19 models and six ResNet34 models. The source-destination pair for each job is selected randomly. The computation capacities of nodes are $s : 200, u : 70, w : 50, v : 50, t : 30$ GFLOPs/s. The link capacity of each link is either 125 or 375MB/s. These capacities are universally scaled down to 0.0001 in order to examine the performance of algorithms with varying link capacities. Fig. 5 shows the job completion times of two algorithms. As the link capacity increases, the job completion time decreases. Intuitively, for sufficiently small transmission delays, the computation time becomes dominant, and it is better for a single inference job to use a single node with highest computation capacity. We observed that with large link capacities, the greedy tends to assign all the layers of a single job to a single node. This shows that our greedy policy (as well as simulated annealing) seeks a routing with small latency. Furthermore, the greedy gives out the result almost instantly while simulated annealing takes a few hundreds of seconds to calculate the (final) solution.

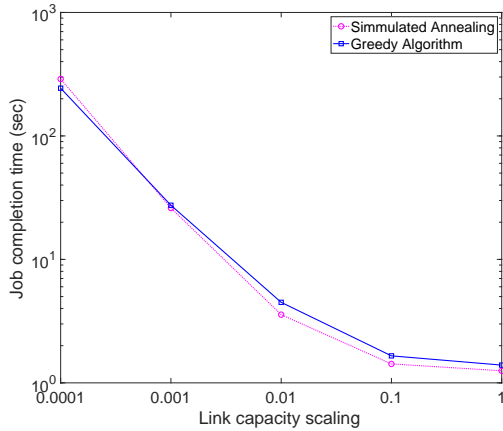


Fig. 5. Job completion time in the small topology. Each point is the average completion time of five different realizations of random src-dst pairs

For the large topology, the computation capacities are [30, 50, 200, 100, 70, 30, 50, 200, 100, 70, 30, 50, 200, 100, 70, 30, 50, 200, 100, 70, 30, 50, 200, 100] GFLOPs/s in the increasing

order of node number in the figure. In addition to the two models used above, we create a new model with the attributes of each layer being manually determined. This model adds the heterogeneity of inference jobs and will help us examine the performance in more diverse environments. There are ten inference jobs ($J = 10$), 6 VGG19, 2 ResNet34 and 2 new models. Similar to the small topology, the source-destination pairs are selected randomly, and this is repeated 5 times for each capacity scaling.

Fig. 5 shows the completion time. In contrast with the small topology, the greedy policy outperforms simulated annealing. Furthermore, as the network size grows, simulated annealing scales poorly as it takes a few tens of minutes in this case while the greedy needs only about 10 seconds to calculate the solution. Considering additional effort needed for determining several parameters in simulated annealing, the results look more convincing for the greedy policy.

VI. CONCLUSION

In this paper, we proposed a framework for routing DNN inference jobs over the distributed computing network. Our framework uses a novel layered graph model to simplify and integrate the communication and computation problems via conventional routing. Our algorithms presented in this paper show an example of what one can do by exploiting the proposed framework. Namely, a simple but effective solution for enjoying the capability of DNN even with the lack of computing power can be derived. In addition to the results in this paper, we believe that our framework can facilitate practical solutions to the problem of routing inference jobs. Our framework will therefore be able to help overcome limited computing power at end devices when ubiquitous AI is about to be in service.

APPENDIX A PROOF OF THEOREM 1

We start with some background needed to show the aforementioned property. The definitions and facts in the following can be found in [15].

Definition 1: An $m \times n$ matrix A is *totally unimodular* (TU) if the determinant of each square submatrix is equal to 0, 1 or -1.

Definition 2: A *polyhedron* $P \subseteq \mathbb{R}^n$ is the set of points that satisfy a finite number of linear inequalities, that is, $P = \{x \in \mathbb{R}^n : Ax \leq b\}$ where $A \in \mathbb{R}^{m \times n}$ and $b \in \mathbb{R}^m$.

Definition 3: A nonempty polyhedron is said to be *integral* if all of its extreme points² are integral.

The following two lemmas are the key to our analysis.

Lemma 1: If $A \in \mathbb{R}^{m \times n}$ is TU, then $P(b) = \{x \in \mathbb{R}_+^n : Ax \leq b\}$ is integral for all $b \in \mathbb{Z}^m$ for which it is nonempty (the same is true for $P(b) = \{x \in \mathbb{R}_+^n : Ax = b\}$).

Lemma 2: For a polyhedron $P \subseteq \mathbb{R}^n$, a solvable LP ($\max\{c^T x : x \in P\}$) has an integral optimal solution for all $c \in \mathbb{R}^n$ if and only if P is integral.

²A point in polyhedron P is extreme if it cannot be expressed as a nontrivial convex combination of two distinct points in P .

By Lemmas 1 and 2, if the constraint matrix is TU, then solving LP with integral vector b in P gives an integral optimal solution (or if not, the fractional solution can be rounded to an integral solution without losing optimality). In the case of binary ILP, LP relaxation replaces the constraints $(\cdot \in \{0, 1\})$ with $(0 \leq \cdot \leq 1)$. If the polyhedron with this relaxation is integral, then solving the LP relaxation gives a binary optimal solution because all the variables are constrained to be between 0 and 1 and hence integrality implies binarity. We exploit this fact to show that LP relaxation of our formulation has a binary optimal solution which in our case is a single path.

A. Matrix Representation of Our Formulation

We first represent the formulation in a matrix form. Let $y = [z; r_1; r_2]^3 \in \mathbb{R}^{(L+1)(|V_p|+|E_p|)}$ where $z = [z_u, \forall u \in V_p] \in \mathbb{R}^{|V_p|}$, $r_1 = [r_{u_l-1 u_l}, \forall u \in V_p, l = 1, 2, \dots, L] \in \mathbb{R}^{L \cdot |V_p|}$ and $r_2 = [r_{uv}, \forall (u, v) \in E_l, l = 0, 1, 2, \dots, L] \in \mathbb{R}^{(L+1) \cdot |E_p|}$. Let A_1 and A_2 be the matrices corresponding to constraints (2) and (3), respectively. Hence, we have $A_1 \in \mathbb{R}^{L \cdot |V_p| \times (L+1)(|V_p|+|E_p|)}$ and $A_2 \in \mathbb{R}^{(L+1) \cdot |V_p| \times (L+1)(|V_p|+|E_p|)}$. The formulation (1)-(5) can be written as

$$\begin{aligned} \min_y \quad & c_1^T y \\ \text{s.t.} \quad & A_1 y \leq 0 \\ & A_2 y = b_2 \\ & y \text{ binary vector} \end{aligned} \quad (6)$$

where c_1 is a vector whose inner product with y gives the service plus waiting time as in (1), and b_2 is a integral vector having 1, -1 or 0.

Lemma 3: LP relaxation of the above formulation can be written as

$$\begin{aligned} \min_y \quad & c^T x \\ \text{subject to} \quad & \begin{bmatrix} A_1 & I_{12} & 0 \\ A_2 & 0 & 0 \\ I_{31} & 0 & I_{33} \end{bmatrix} \begin{bmatrix} y \\ s_1 \\ s_2 \end{bmatrix} = \begin{bmatrix} 0 \\ b_2 \\ 1 \end{bmatrix} \\ & y, s_1, s_2 \geq 0 \end{aligned} \quad (7)$$

where x is the vector $[y; s_1; s_2]$, and $s_1 \in \mathbb{R}^{(L+1)(|V_p|+|E_p|)}$ and $s_2 \in \mathbb{R}^{L \cdot |V_p|}$ are slack variables. The vector c is the augmented vector of c_1 in (6) padded with zero to match the dimension of x . The matrices I_{mn} are identity matrices of appropriate sizes.

Proof: To replace inequality constraint in (6) with equality constraint, we introduce the slack variable $s_1 \geq 0$. The formulation (6) is equivalent to

$$\begin{aligned} \min \quad & c_1^T y \\ \text{s.t.} \quad & A_1 y + s_1 = 0 \\ & A_2 y = b_2 \\ & y \text{ binary vector} \\ & s_1 \geq 0 \end{aligned} \quad (8)$$

³The notation $;$ is used to indicate the beginning of a new row. For example, $[1; -1; 1]$ is a 3-dimensional column vector.

Now relax the binarity constraint as

$$\begin{aligned} \min \quad & c_1^T y \\ \text{s.t.} \quad & A_1 y + s_1 = 0 \\ & A_2 y = b_2 \\ & y \leq 1 \\ & y, s_1 \geq 0 \end{aligned} \quad (9)$$

The slack variable s_2 is introduced to replace the inequality constraint with equality constraint again, i.e., replace $y \leq 1$ with $y + s_2 = 1$ and $s_2 \geq 0$. Putting all the equality constraints together obtains the desired result (7). ■

Note that the polyhedron in LP relaxation (7) is the same form as in Lemma 1 with equality $Ax = b$, where

$$A = \begin{bmatrix} A_1 & I_{12} & 0 \\ A_2 & 0 & 0 \\ I_{31} & 0 & I_{33} \end{bmatrix}, \quad x = \begin{bmatrix} y \\ s_1 \\ s_2 \end{bmatrix}, \quad b = \begin{bmatrix} 0 \\ b_2 \\ 1 \end{bmatrix} \quad (10)$$

Note that b is an integral vector. Consequently, by Lemmas 1 and 2, we just need to show the total unimodularity of A .

B. Total Unimodularity

We start with some background on total unimodularity [15].

Lemma 4: For an $m \times n$ integral matrix A , the following are equivalent:

- 1) A is TU
- 2) A^T is TU
- 3) For each $C \subseteq \{1, \dots, n\}$, there exists a partition (C_1, C_2) of C such that

$$\left| \sum_{j \in C_1} a_{ij} - \sum_{j \in C_2} a_{ij} \right| \leq 1 \text{ for } i = 1, \dots, m \quad (11)$$

- 4) For each $R \subseteq \{1, \dots, m\}$, there exists a partition (R_1, R_2) of R such that

$$\left| \sum_{i \in R_1} a_{ij} - \sum_{i \in R_2} a_{ij} \right| \leq 1 \text{ for } j = 1, \dots, j \quad (12)$$

Condition (11) requires that for each row, the partitioned sum (called partitioned row sum) must differ by at most 1. Note that statement 4) in Lemma 4 is an immediate consequence of 1), 2) and 3).

We can show the following lemma.

Lemma 5: If $[A_1; A_2]$ is TU, then A is TU.

Proof: Suppose that $[A_1; A_2]$ is TU. Then, by statement 3) in Lemma 4, any subset of the first block column (i.e., block containing $[A_1; A_2]$) can be partitioned into two sets C_1 and C_2 so that condition (11) is satisfied. Note that the identity matrix I_{31} in the first block column of A does not affect the forming of C_1 and C_2 because any column partition of identity matrix satisfies condition (11).

Next, consider adding an arbitrary column, say i th column, from the second block column of A . Note that the only nonzero entry (which is 1) is in the i th row of this column. So, if the current partitioned sum difference of i th row is zero, then put the column into either C_1 or C_2 , which does not violate

condition (11). If the partitioned row sum difference is 1, put the column into a subset with smaller row sum so that the partitioned row sum difference is balanced, i.e., zero. The third block column can be treated exactly the same as the second block in order to keep the condition in (11). This completes the proof. \blacksquare

We can now focus on proving the total unimodularity of $[A_1; A_2]$ which is indeed totally unimodular.

Lemma 6: The matrix $[A_1; A_2]$ is TU.

Proof: Consider the breakdown of $[A_1; A_2]$ as shown in Fig. 6. Let $A_1 = [A_{11} \ A_{12} \ A_{13}]$. The first $|V_p|$ columns correspond to the variables $z_u, \forall u \in V_p$. The next $L|V_p|$ columns correspond to the variables $r_{u_l-1u}, \forall l = 1, \dots, L, \forall u \in V_p$. The last $(L+1)|E_p|$ columns correspond to the variables $r_{uv}, \forall (u, v) \in E_l, l = 0, 1, \dots, L$.

Each row of A_1 in the top block corresponds to a constraint in (2). Constraints are arranged such that the first block of L rows corresponds to some node u , and each row in the block indicates whether each cross-layer edge along replicated nodes of u is visited. This is repeated for every other node in V_p . This forms the matrix A_1 .

Each row of A_2 in the bottom block corresponds to a flow conservation constraint in (3). For instance, for some node $u \in V_p$, the first $L + 1$ rows correspond to the flow conservation at replicated nodes u_l in each layer $l = 0, 1, \dots, L$. As in A_1 , the second block A_{22} corresponds to the variables $r_{u_{l-1}u_l}, l = 1, \dots, L$ of cross-layer edges. Constraints are arranged in the order of u_0, u_1, \dots, u_L . Since the edges are between consecutive nodes, A_{22} are written as in Fig. 6. Note that this A_{22} is a network matrix. The third block A_{23} corresponds to the variables $r_{uv}, \forall (u, v) \in E_l, l = 0, 1, \dots, L$ of intra-layer edges. Clearly, A_{23} is a network matrix of $L + 1$ connected components G_0, \dots, G_L .

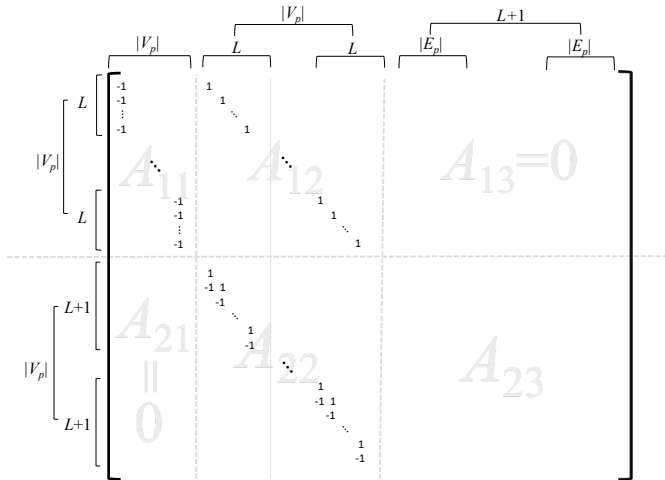


Fig. 6. Breakdown of matrix A . A_{23} is the network matrix of $L + 1$ layers G_0, \dots, G_L without cross-layer edges

Consider partitioning the columns of the matrix A . Let C_1 and C_2 be a partition of an arbitrary subset C of the entire columns. The following rule is applied for the partition.

- 1) Put any column from the first $(L+1)|V_p|$ columns into C_1 regardless of J
 - Without the third column block (i.e., the columns of $[A_{13}; A_{23}]$, this guarantees that each row sum is 0, 1, or -1 . Furthermore, the row sums corresponding to A_{22} have exactly the same numbers of 1s and -1 s. Let $s \in \mathbb{R}^{(L+1)|V_p|}$ be the vector of these row sums from the columns of A_{22} . Again, s has exactly same numbers of 1s and -1 s. Consider the matrix $[s \ A_{23}]$. This matrix is obviously TU because i) s has exactly the same numbers of 1s and -1 s and ii) each column of A_{23} has exactly one 1 and one -1 . Consequently, any subset of rows can be partitioned into two subsets so that the condition in (12) can be satisfied. That partition is indeed putting all the rows in the same subset, with which the partitioned column sum difference is always 0, 1, or -1 . Consequently, $[s \ A_{23}]$ is TU and any subset of columns of the matrix can be partitioned so that the condition in (11) is satisfied.
- 2) Treat any columns from the first two block columns as a single column by adding those columns. Let d be the resulting column vector. Let E be the matrix of arbitrary column(s) from $[A_{13}; A_{23}]$. Partition the columns of $[d \ E]$ in the same way as partitioning an arbitrary subset of columns of $[s, A_{23}]$ discussed above.
 - As shown in 1), all of the top block row sums satisfy condition (11) since the third block column in the top block row (i.e., A_{13}) is a zero matrix. By the argument in 1) on the TU of $[s \ A_{23}]$, all of the bottom block row sums also satisfy (11).

This completes the proof. \square

Proof of Theorem 2: By Lemmas 6 and 5, A is TU. By Lemmas 2 and 1, LP relaxation (7) has an integral optimal solution. It is clear that LP relaxation (7) is equivalent to (13).

$$\begin{aligned} \min \quad & c_1^T y \\ \text{s.t.} \quad & A_1 y \leq 0 \\ & A_2 y = b_2 \\ & 0 \leq y \leq 1 \end{aligned} \tag{13}$$

Therefore, LP relaxation (13) has an integral optimal solution which is a single path with minimum completion time.

APPENDIX B

PROOF OF THEOREM 2

We first introduce various routing policies below.

- Shortest completion (SC): optimal routing policy that achieves minimum job completion time in the actual system
- Shortest service (SS): routing policy that achieves shortest service time
- Greedy (GR): Algorithm 1
- Shortest waiting (SW): given that $p - 1$ jobs are routed by greedy, the p th job is assigned to a node with positive

computation capacity, say u^* , with shortest computation waiting time. Then, a shortest transmission waiting path is assigned from source to u^* and from u^* to destination.

The following notation is used:

- W_j^π : total waiting time of job j under routing policy π
- S_j^π : total service time of job j under routing policy π
- $W_j^\pi(tx)$: total transmission waiting time of job j under routing policy π
- $W_j^\pi(cp)$: total computation waiting time of job j under routing policy π
- $S_j^\pi(tx)$: total transmission (service) time of job j under routing policy π
- $S_j^\pi(cp)$: total computation (service) time of job j under routing policy π

It is clear from the definition that $W_j^\pi + S_j^\pi$ is the completion time of job j under routing policy π . We also have $S_j^\pi = S_j^\pi(tx) + S_j^\pi(cp)$ and $W_j^\pi = W_j^\pi(tx) + W_j^\pi(cp)$.

We need a few lemmas to prove Theorem 2. For simplicity of presentation, we break the results into small lemmas and integrate these results for the proof of Theorem 2. Denote by j_p the p th job routed under greedy routing policy.

Lemma 7: The job completion time under greedy algorithm is $W_{j_J}^{GR} + S_{j_J}^{GR}$ where j_J is the last job routed under greedy algorithm.

Proof: The greedy policy routes a job with earlier completion time first, and hence, the waiting time plus service time of last job routed under greedy is the job completion time of the greedy policy. ■

Consequently, in order to analyze the job completion time of greedy policy, we just need to derive a bound on $W_{j_J}^{GR} + S_{j_J}^{GR}$.

Lemma 8: The optimal job completion time T^* is lower-bounded as

$$S_j^{SS} \leq T^*, j = 1, \dots, J \quad (14)$$

$$\frac{1}{|V_p| + |E_p|} \sum_{j=1}^J S_j^{SS} \leq T^* \quad (15)$$

Proof: The LHS in inequality (14) is the fastest possible service time of job j . The entire job is completed only after every job has been served. Hence, the minimum completion time T^* cannot be smaller than the fastest possible service time of every job.

To show (15), we have

$$\frac{1}{|V_p| + |E_p|} \sum_{j=1}^J S_j^{SS} \leq \frac{1}{|V_p| + |E_p|} \sum_{j=1}^J S_j^{SC} \leq T^* \quad (16)$$

The first inequality holds since the total service time of SC cannot be smaller than that of SS. In the second inequality, the LHS is the average busy time of network components (nodes+links) under SC. It is clear that job cannot be completed as long as there remains a busy component under SC, and consequently, optimal job completion time T^* is no smaller than the LHS. Note that the service time at the link with infinite capacity is zero, and hence, those links should be excluded when computing the average. Similarly, under

SS or SC, the computation will not be carried out at the node with zero computation capacity, and hence, those nodes should be excluded when computing the average. This completes the proof. ■

The above lemma enables to compare GR and SC via SS. Let h_L^j and h_S^j be the longest and shortest path lengths in hop count between s^j and t^j , respectively. Define $h_L = \max_j h_L^j$ and $h_S = \max_j h_S^j$.

Lemma 9: The transmission times are bounded as

$$S_j^{SW}(tx) \leq 2\alpha_{tx} S_j^{SS}(tx), \forall j \quad (17)$$

$$S_j^{GR}(tx) \leq (L+1)\alpha_{tx} S_j^{SS}(tx), \forall j \quad (18)$$

where $\alpha_{tx} = \frac{h_L \cdot \max_{j,l} d_{jl} \cdot \max_{(u,v)} \mu_{uv}}{h_S \cdot \min_{j,l} d_{jl} \cdot \min_{(u,v)} \mu_{uv}}$.

Proof: Under routing policy SW, link transmission occurs only in layers 0 and L because all the NN layers are computed in a single node with smallest computation waiting time. Furthermore, in layers 0 and L , the transmission path is simple because it takes a shortest transmission waiting path. Consequently, in both of layers 0 and L , the transmission time is at most $\frac{h_L \cdot \max_l d_l}{\min_{(u,v)} \mu_{uv}}$. The transmission time under SW is thus upper-bounded as

$$S_j^{SW}(tx) \leq 2 \frac{h_L \cdot \max_l d_l}{\min_{(u,v)} \mu_{uv}}. \quad (19)$$

On the other hand, the transmission time under SS is at least $\frac{h_S \cdot \min_{j,l} d_{jl}}{\max_{(u,v)} \mu_{uv}}$. Combining this with inequality in (19) yields the desired result (17).

To prove (18), the same argument as above is applied to each of $L+1$ layers in G since the greedy policy finds a simple path in each layer. This completes the proof. ■

Lemma 10: For any routing policy π , the computation service time is upper-bounded as

$$S_j^\pi(cp) \leq \alpha_{cp} S_j^{SS}(cp), \forall j \quad (20)$$

where $\alpha_{cp} = \frac{\max_u \mu_u}{\min_u \mu_u}$.

Proof: The worst case is when all the layers are computed at the node with smallest (positive) computation capacity, and the best case is when computed at the node with largest computation capacity. The lemma immediately follows from this observation. ■

Lemma 11: The service time under routing policy SW is bounded as

$$S_j^{SW} \leq \alpha_1 T^*, \forall j, \quad (21)$$

where $\alpha_1 = \max(2\alpha_{tx}, \alpha_{cp})$.

Proof: We have

$$S_j^{SW} = S_j^{SW}(tx) + S_j^{SW}(cp) \quad (22)$$

$$\leq 2\alpha_{tx} S_j^{SS}(tx) + \alpha_{cp} S_j^{SS}(cp) \quad (23)$$

$$\leq \alpha_1 T^* \quad (24)$$

The first inequality follows from Lemma 9, and the second inequality follows from Lemma 10. ■

The above lemmas characterize the bounds on the service time. We now derive the bounds on the waiting time. Recall that given $p-1$ jobs routed by GR, the policy SW routes the p th job j_p as above.

Lemma 12: Suppose that the original graph G_p is k -edge-connected. Then,

$$W_{j_J}^{SS}(tx) \leq \frac{2(L+1)\alpha_{tx}}{k} \sum_{p=1}^{J-1} S_{j_p}^{SS}(tx). \quad (25)$$

Proof: Recall that when job j_J is to be routed by SW, the rest of $J-1$ jobs have already been routed by GR. By assumption, there are k disjoint paths between any pair of nodes. For the path segment from source to u^* , the average transmission waiting time along each of k disjoint paths is at most⁴ $\frac{1}{k} \sum_{p=1}^{J-1} S_{j_p}^{GR}(tx)$. This shows that there is a path from source to u^* with transmission waiting time no greater than $\frac{1}{k} \sum_{p=1}^{J-1} S_{j_p}^{GR}(tx)$. Since the routing policy SW selects a path from source to u^* that has the smallest transmission waiting time, the transmission waiting time $W_{j_J}^{SN}(tx)$ is upper-bounded by $\frac{1}{k} \sum_{p=1}^{J-1} S_{j_p}^{GR}(tx)$. By Lemma 9, this is in turn upper-bounded by $\frac{(L+1)}{k} \sum_{p=1}^{J-1} S_{j_p}^{SS}(tx)$. Applying the same argument to the segment from u^* to destination proves the lemma. ■

Lemma 13: We have

$$W_{j_J}^{SW}(cp) \leq \frac{\alpha_{cp}}{|V_p|} \sum_{p=1}^{J-1} S_{j_p}^{SS}(cp) \quad (26)$$

Proof: This lemma immediately follows from the following inequalities:

$$W_J^{SW}(cp) \leq \frac{1}{|V_p|} \sum_{j=1}^{J-1} S_j^{GR}(cp) \leq \frac{\alpha_{cp}}{|V_p|} \sum_{j=1}^{J-1} S_j^{SS}(cp) \quad (27)$$

Recall that both GR (by nature of formulation (1)-(4)) and SW (by definition) do not compute at the node with zero computation capacity. In addition, $|V_p|$ is the number of nodes with positive computation capacity. The RHS of the first inequality is thus the average computation waiting time at a node. Since the routing policy SW selects a node with minimum waiting time, the node waiting time under SW should be no greater than the average node waiting time, which shows the first inequality. The second inequality follows from Lemma 10. This completes the proof. ■

Lemma 14: We have

$$W_{j_J}^{GR} + S_{j_J}^{GR} \leq W_{j_J}^{SW} + S_{j_J}^{SW}. \quad (28)$$

Proof: Recall that given $J-1$ jobs routed by GR, SW finds a path such that the last job is processed at a single node,

say u^* , with minimum waiting time, and a shortest (in link transmission waiting) path from source to u^* and a shortest path from u^* to destination are concatenated to form a path from source to destination of the last job. On the other hand, for the last job, GR finds a path with minimum waiting plus service time, given $J-1$ jobs routed by GR. Therefore, the inequality holds. ■

Proof of Theorem 2: By Lemmas 7 and 14, the job completion time under GR is at most $W_{j_J}^{SW} + S_{j_J}^{SW}$. Let $\alpha_2 = \max\left(\frac{\alpha_{cp}}{|V_p|}, \frac{2(L+1)\alpha_{tx}}{k}\right)$. By Lemmas 12 and 13, we have

$$W_{j_J} \leq \frac{\alpha_{cp}}{|V_p|} \sum_{p=1}^{J-1} S_{j_p}^{SS}(cp) + \frac{2(L+1)}{k} \sum_{p=1}^{J-1} S_{j_p}^{SS}(tx) \quad (29)$$

$$\leq \alpha_2 \sum_{p=1}^{J-1} S_{j_p}^{SS} \quad (30)$$

This together with Lemma 11 leads to

$$W_{j_J}^{SW} + S_{j_J}^{SW} \leq \alpha_2 \sum_{p=1}^{J-1} S_{j_p}^{SS} + \alpha_1 S_{j_J}^{SS} \quad (31)$$

$$\leq \alpha_3 \left\{ \frac{1}{|V_p| + |E_p|} \sum_{p=1}^{J-1} S_{j_p}^{SS} + S_{j_J}^{SS} \right\} \quad (32)$$

$$= \alpha_3 \left\{ \frac{1}{|V_p| + |E_p|} \sum_{p=1}^J S_{j_p}^{SS} + \left(1 - \frac{1}{|V_p| + |E_p|}\right) S_{j_J}^{SS} \right\} \quad (33)$$

$$\leq \alpha_3 \left(2 - \frac{1}{|V_p| + |E_p|}\right) T^* \quad (34)$$

where $\alpha_3 = \max(\alpha_2(|V_p| + |E_p|), \alpha_1)$. The last inequality follows from Lemma 8. This completes the proof

APPENDIX C

PROOF OF COROLLARY 1

By assumption of zero network delay, $|E_p| = 0$ and $\alpha_{tx} = 0$ (this is because Lemma 8 holds with $\alpha_{tx} = 0$). In addition, $\alpha_{cp} = 1$. It immediately follows that $\alpha = 2 - \frac{1}{|V_p| + |E_p|}$, completing the proof.

REFERENCES

- [1] K. B. Letaief, W. Chen, Y. Shi, J. Zhang, and Y.-J. A. Zhang, "The Roadmap to 6G: AI Empowered Wireless Networks," *IEEE Communications Magazine*, vol. 57, no. 8, pp. 84–90, 2019.
- [2] F. N. Iandola, M. W. Moskewicz, K. Ashraf, S. Han, W. J. Dally, and K. Keutzer, "SqueezeNet: AlexNet-level accuracy with 50x fewer parameters and <1MB model size," *CoRR*, vol. abs/1602.07360, 2016. [Online]. Available: <http://arxiv.org/abs/1602.07360>
- [3] A. G. Howard, M. Zhu, B. Chen, D. Kalenichenko, W. Wang, T. Weyand, M. Andreetto, and H. Adam, "MobileNets: Efficient Convolutional Neural Networks for Mobile Vision Applications," *CoRR*, vol. abs/1704.04861, 2017. [Online]. Available: <http://arxiv.org/abs/1704.04861>
- [4] A. Howard, M. Sandler, B. Chen, W. Wang, L.-C. Chen, M. Tan, G. Chu, V. Vasudevan, Y. Zhu, R. Pang, H. Adam, and Q. Le, "Searching for mobilenetv3," in *2019 IEEE/CVF International Conference on Computer Vision (ICCV)*, 2019, pp. 1314–1324.
- [5] P. Ren, Y. Xiao, X. Chang, P.-y. Huang, Z. Li, X. Chen, and X. Wang, "A comprehensive survey of neural architecture search: Challenges and solutions," vol. 54, no. 4, 2021. [Online]. Available: <https://doi.org/10.1145/3447582>

⁴This is an upper bound as there may edges not in k disjoint paths.

- [6] E. Di Pascale, I. Macaluso, A. Nag, M. Kelly, and L. Doyle, "The Network As a Computer: A Framework for Distributed Computing Over IoT Mesh Networks," *IEEE Internet of Things Journal*, vol. 5, no. 3, pp. 2107–2119, 2018.
- [7] E. Baccour, A. Erbad, A. Mohamed, M. Hamdi, and M. Guizani, "RL-PDNN: Reinforcement Learning for Privacy-Aware Distributed Neural Networks in IoT Systems," *IEEE Access*, vol. 9, pp. 54 872–54 887, 2021.
- [8] S. Disabato, M. Roveri, and C. Alippi, "Distributed Deep Convolutional Neural Networks for the Internet-of-Things," *IEEE Transactions on Computers*, vol. 70, no. 8, pp. 1239–1252, 2021.
- [9] Z. Zhao, K. M. Barijough, and A. Gerstlauer, "DeepThings: Distributed Adaptive Deep Learning Inference on Resource-Constrained IoT Edge Clusters," *IEEE Transactions on Computer-Aided Design of Integrated Circuits and Systems*, vol. 37, no. 11, pp. 2348–2359, 2018.
- [10] Y. Chang, X. Huang, Z. Shao, and Y. Yang, "An Efficient Distributed Deep Learning Framework for Fog-Based IoT Systems," in *2019 IEEE Global Communications Conference (GLOBECOM)*, 2019, pp. 1–6.
- [11] M. R. Garey and D. S. Johnson, *Computers and Intractability: A Guide to the Theory of NP-Completeness*. USA: W. H. Freeman & Co., 1990.
- [12] Z. Cao, S. S. Panwar, M. Kodialam, and T. V. Lakshman, "Enhancing mobile networks with software defined networking and cloud computing," *IEEE/ACM Transactions on Networking*, vol. 25, no. 3, pp. 1431–1444, 2017.
- [13] J. Zhang, A. Sinha, J. Llorca, A. M. Tulino, and E. Modiano, "Optimal control of distributed computing networks with mixed-cast traffic flows," *IEEE/ACM Transactions on Networking*, vol. 29, no. 4, pp. 1760–1773, 2021.
- [14] P. Molchanov, S. Tyree, T. Karras, T. Aila, and J. Kautz, "Pruning convolutional neural networks for resource efficient inference," in *5th International Conference on Learning Representations, ICLR 2017, Toulon, France, April 24-26, 2017, Conference Track Proceedings*. OpenReview.net, 2017. [Online]. Available: <https://openreview.net/forum?id=SJGCiw5gl>
- [15] G. L. Nemhauser and L. A. Wolsey, *Integer and Combinatorial Optimization*. New York, NY, USA: Wiley-Interscience, 1999.